

## Discovery of a Potent, Nonpolyglutamatable Inhibitor of Glycinamide Ribonucleotide Transformylase

Jessica K. DeMartino, Inkyu Hwang, Lan Xu, Ian A. Wilson, and Dale L. Boger\*

Departments of Chemistry, Molecular Biology, and The Skaggs Institute for Chemical Biology, The Scripps Research Institute, 10550 North Torrey Pines Road, La Jolla, California 92037

Received February 2, 2006

Glycinamide ribonucleotide transformylase (GAR Tfase) catalyzes the first of two formyl transfer steps in the de novo purine biosynthetic pathway that require folate cofactors. Herein we report the discovery of a potent, nonpolyglutamatable, and selective inhibitor of GAR Tfase. Compound **12**, which possesses a tetrazole in place of the  $\gamma$ -carboxylic acid in the L-glutamate subunit of the potent GAR Tfase inhibitor **1**, was active in cellular-based functional assays exhibiting purine-sensitive cytotoxic activity ( $IC_{50} = 40$  nM, CCRF-CEM) and was selective for inhibition of rhGAR Tfase ( $K_i = 130$  nM). Notably, **12** was only 2.5-fold less potent than **1** in cellular assays and 4-fold less potent against rhGAR Tfase. Like **1**, this functional activity of **12** in the cell-based assay benefits from and requires transport into the cell by the reduced folate carrier but, unlike **1**, is independent of folyl polyglutamate synthase (FPGS) expression levels and polyglutamation.

### Introduction

Glycinamide ribonucleotide transformylase (GAR Tfase) is a folate-dependent enzyme central to the de novo purine biosynthetic pathway,<sup>1,2</sup> and it utilizes the cofactor 10-formyltetrahydrofolic acid (10-formyl-THF) to transfer a formyl group to the primary amine of its substrate  $\beta$ -glycinamide ribonucleotide ( $\beta$ -GAR). Potent, and potentially selective, inhibitors of GAR Tfase and de novo purine biosynthesis have shown promise as antitumor drugs. Although the rationale for the oncology use of a selective purine biosynthesis inhibitor has often been questioned, the disclosures that many tumors lack methylthioadenosine phosphorylase (MTAP)<sup>3,4</sup> and the capacity found in normal cells for the salvage pathway synthesis of purines have suggested that such tumors would be uniquely sensitive to selective inhibitors of de novo purine biosynthesis.<sup>5,6</sup> Moreover, the clinical success of antifolates that inhibit multiple folate-dependent enzymes found in both the purine and pyrimidine biosynthetic pathways have contributed to the perception that a pure purine biosynthesis inhibitor may not be as attractive.<sup>7</sup> Complicating the analysis of such antifolates is the fact that most act as their polyglutamate conjugates which exhibit enhanced affinities for most folate-dependent enzymes making it difficult to unambiguously establish relationships between target inhibition and functional activity. The work detailed herein provides an unusually potent and selective purine biosynthesis inhibitor that acts by inhibiting GAR Tfase and that is incapable of polyglutamation, making it ideally suited to directly address such questions.

Just as significantly, classical inhibitors of folate-dependent enzymes including methotrexate and lometrexol suffer from issues relating to polyglutamation (Figure 1). Long-term exposure to methotrexate and pemetrexed leads to down-regulation of folypolyglutamate synthase (FPGS) and the emergence of a resistant phenotype,<sup>8,9</sup> while lometrexol suffers from cumulative toxicity requiring coadministration of folic acid.<sup>10</sup> This cumulative toxicity of antifolates such as lometrexol is thought to result from the inability of cells to efflux inhibitors due to their polyglutamated state. FPGS converts monoglutamate folates or

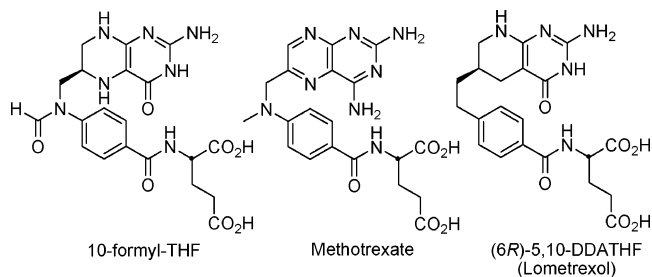


**Figure 1.** Cofactor and representative inhibitors of folate-dependent enzymes.

antifolates to their polyglutamate forms (2–9 additional  $\gamma$ -glutamates) once they enter the cell, and this glutamation only occurs at the  $\gamma$ -position and not the  $\alpha$ -position. The polyglutamated compounds generally bind better to their respective enzymes, and they are less capable or incapable of being transported out of the cell.<sup>11</sup> Although such polyglutamation may be beneficial for increasing target enzyme affinity or for increasing intracellular accumulation, it also places limitations on the antifolate. Tumor cell down-regulation of FPGS, which may be either inherent or acquired, leads to resistance against classical antifolates that benefit from polyglutamation.<sup>8,9</sup> In such instances, efficacious antifolates that do not depend on or that lack the ability to be polyglutamated may prove useful in the treatment of antifolate-resistant tumors whose resistance is derived from reduced FPGS activity, and they may exhibit a reduced normal cell toxicity.<sup>12–18</sup>

In previous studies, we reported the synthesis and biological evaluation of **1**, 10-trifluoroacetyl-DDACTHF (10-CF<sub>3</sub>CO-DDACTHF),<sup>19</sup> the most potent GAR Tfase inhibitor described to date ( $IC_{50} = 16$  nM, CCRF-CEM;  $K_i = 15$  nM, rhGAR Tfase) (Figure 2). In the case of **1**, it was found that its potent, purine-sensitive cytotoxic activity benefited from FPGS polyglutamation which appeared to be related to an enhanced intracellular accumulation (due to polyglutamation) and not enhanced enzyme inhibitory potency.<sup>20</sup>

As a result, two derivatives of **1** were prepared incorporating  $\alpha$ - and  $\gamma$ -carboxamides in place of the L-glutamate carboxylic acids<sup>21</sup> to provide further insight into the role of the glutamate subunit and polyglutamation for activity. The L-glutamine

\* To whom correspondence should be addressed. Phone (858)784-7522. Fax: (858)784-7550. E-mail: boger@scripps.edu.

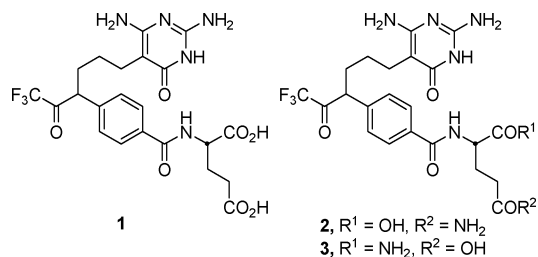


Figure 2. Inhibitors of GAR Tfase.

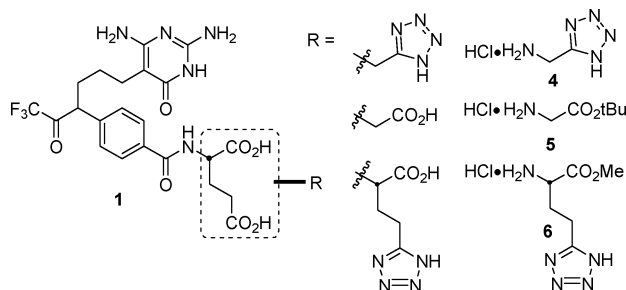


Figure 3. Side chain modifications.

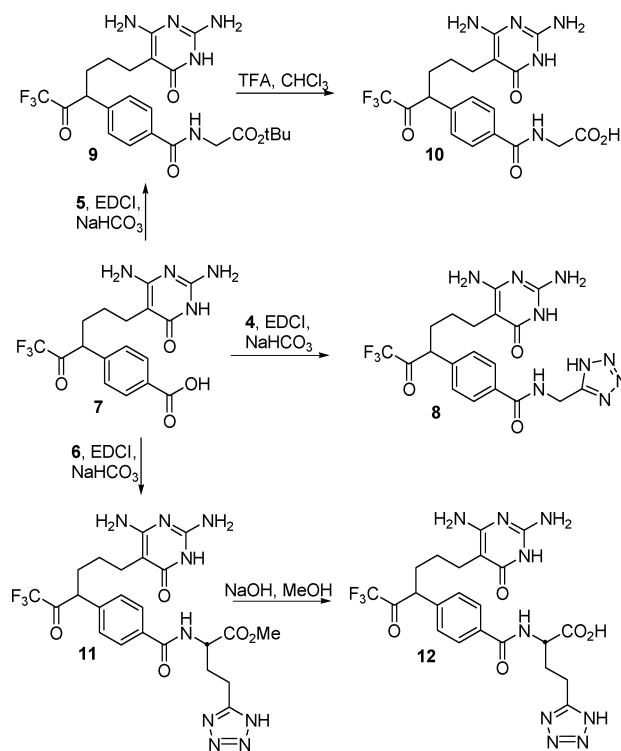
derivative **2** was found to be a potent and selective inhibitor of rhGAR Tfase ( $K_i = 56$  nM) and surprisingly active in cellular assays exhibiting purine-sensitive cytotoxic activity ( $IC_{50} = 300$  nM). As anticipated, this masking of the L-glutamate  $\gamma$ -carboxylic acid as a carboxamide had little impact on the enzyme inhibitory activity, but it also had less of an effect on the functional (cellular) activity than expected despite its blockage of FPGS polyglutamation as well as its potential impact on reduced folate carrier transport into the cell. In contrast, and as anticipated, the L-isoglutamine derivative **3** was much less effective as a rhGAR Tfase inhibitor ( $K_i = 4.8$   $\mu$ M) and was inactive in the cellular assays. This loss of activity with **3** reflects the critical contact the L-glutamate  $\alpha$ -carboxylic acid makes at the enzyme active site,<sup>19</sup> as well as the influence it might have on both FPGS polyglutamation and reduced folate carrier transport. Of these observations, it was surprising that **2** was only 20-fold less potent than the parent compound **1** in functional (cellular) assays, and it was not clear whether this was simply a consequence of preventing polyglutamation or the result of a less effective transport by the reduced folate carrier. Thus, the surprisingly potent activity of **2** suggested that selective and efficacious GAR Tfase inhibitors that do not require FPGS polyglutamation might be accessible provided they were designed to be effectively transported by the reduced folate carrier.

Herein we report the synthesis and evaluation of three such derivatives of 10-CF<sub>3</sub>CO-DDACTHF (**1**) that incorporate **4–6** in place of the L-glutamate subunit, which were expected to preclude their ability to serve as substrates for FPGS polyglutamation (Figure 3).

### Inhibitor Synthesis

The candidate inhibitors were prepared from the common precursor **7** (Scheme 1).<sup>21</sup> Carboxylic acid **7** was coupled with each side chain<sup>14,22</sup> (**4**, **5**, and **6**) indicated in Figure 3 using 1-(3-dimethylaminopropyl)-3-ethylcarbodiimide (EDCI) and sodium bicarbonate, to afford the coupled products **8**, **9**, and **11**. Inhibitor **8** needed no further modification, while compounds **9** and **11** were deprotected under acidic and basic conditions, respectively, to give the final compounds **10** and **12**. The candidate inhibitors and synthetic intermediates **7–12** constitute a mixture of *R* and *S* configurations at the trifluoroacetyl center

### Scheme 1

Table 1. GAR and AICAR Tfase Inhibition ( $K_i$ ,  $\mu$ M)

| compd      | rhGAR Tfase       | rhAICAR Tfase |
|------------|-------------------|---------------|
| <b>8</b>   | 5.0               | >100          |
| <b>10</b>  | 21.0              | >100          |
| <b>12</b>  | 0.13              | 46            |
| <b>1</b>   | 0.03              | >100          |
| lometrexol | 0.06 <sup>a</sup> | >100          |

<sup>a</sup> Ref 25.

(enantiomers for **7–10**, diastereomers for **11** and **12**). Like **1–3**, the diastereomers for **11** and **12** were not chromatographically separable and the configuration at C10 appears to readily interconvert.

### Results and Discussion

Compounds **8**, **10**, and **12** were tested for inhibition of GAR Tfase and aminoimidazole carboxamide ribonucleotide transformylase (AICAR Tfase), and the results are presented in Table 1. Consistent with the design, **12** proved to be a potent inhibitor of rhGAR Tfase ( $K_i = 130$  nM), being only 4-fold less active than **1** ( $K_i = 30$  nM; lit.<sup>19</sup>  $K_i = 15$  nM) when the two inhibitors were examined side-by-side, and **12** exhibited very modest inhibition of rhAICAR Tfase ( $K_i = 46$   $\mu$ M). In contrast, both **8** and **10** were much less effective (50–100-fold) against rhGAR Tfase ( $K_i = 5.0$  and  $21$   $\mu$ M, respectively) and both were inactive against rhAICAR Tfase ( $K_i > 100$   $\mu$ M).

Compounds **8**, **10**, and **12** were also examined for cytotoxic activity (growth inhibition) both in the presence (+) and absence (–) of added hypoxanthine (purine) or thymidine (pyrimidine) against the CCRF–CEM cell line (Table 2). Of the three inhibitors, only **12** exhibited potent activity in this cell-based assay ( $IC_{50} = 40$  nM). Moreover, **12** differs only by a factor of 2.5 from the lead compound **1** ( $IC_{50} = 16$  nM) and is 5-fold more potent than lometrexol despite the fact that it is incapable of FPGS polyglutamation. In the presence of thymidine, a pyrimidine, the activity of **12** was unaltered, whereas the

**Table 2.** In Vitro Cytotoxic Activity

| compd      | CCRF-CEM (IC <sub>50</sub> , μM) |                 |                 |
|------------|----------------------------------|-----------------|-----------------|
|            | (-) T,<br>(-) H                  | (+) T,<br>(-) H | (-) T,<br>(+) H |
| <b>8</b>   | 10                               | 30              | >100            |
| <b>10</b>  | >100                             | >100            | >100            |
| <b>12</b>  | 0.040                            | 0.090           | >100            |
| <b>1</b>   | 0.016                            | 0.017           | >100            |
| lometrexol | 0.2                              | 0.2             | >100            |

**Table 3.** In Vitro Cytotoxic Activity in Mutant Cell Lines

| compd      | IC <sub>50</sub> , μM [(-)T, (-)H] |                                |                        |
|------------|------------------------------------|--------------------------------|------------------------|
|            | CCRF-CEM                           | CCRF-CEM/<br>FPGS <sup>-</sup> | CCRF-CEM/<br>MTX       |
| <b>8</b>   | 10                                 | 40                             | 30                     |
| <b>10</b>  | >100                               | >100                           | >100                   |
| <b>12</b>  | 0.040                              | 0.050                          | 10                     |
| <b>1</b>   | 0.016                              | >100                           | >100                   |
| lometrexol | 0.2                                | 25 (>100) <sup>a</sup>         | nd (>100) <sup>a</sup> |

<sup>a</sup> Ref 25.

coadministration of hypoxanthine, a purine, rescued cell growth. This indicates that **12**, like **1**, acts by selectively inhibiting an enzyme within the purine, and not pyrimidine, biosynthetic pathway consistent with its potent inhibition of rhGAR Tfase. Compounds **8** and **10** showed little to no activity (IC<sub>50</sub> > 100 μM and 30 μM, respectively). Notably, the comparable functional (cellular) activity of **12** relative to that of its parent **1** suggests that it is effectively transported into the cell even with the glutamate modification and that its intracellular functional activity is independent of FPGS.

Thus, all three inhibitors were subsequently examined in mutant CCRF-CEM cell lines that lack FPGS (CCRF-CEM/FPGS<sup>-</sup>) or the reduced folate carrier (CCRF-CEM/MTX) (Table 3). Like **1**, the cytotoxic activity of **12** in the cell line deficient in the reduced folate carrier (CCRF-CEM/MTX) was greatly diminished (>250-fold) indicating that it benefits from and requires reduced folate carrier transport into the cell. Unlike **1** and lometrexol, the activity of **12** was unaffected in the cell line deficient in FPGS indicating that it does not require or benefit from FPGS polyglutamation. As might be anticipated, the functional activity of both **8** and **10** (essentially inactive) was relatively unaffected in these cell lines. These results illustrate that the functional activity of **12** requires the reduced folate carrier suggesting that **12** is a substrate for and is transported into the cell by the reduced folate carrier and, as anticipated, that FPGS does not affect the activity. Thus, conversion of the glutamate  $\gamma$ -carboxylic acid to a tetrazole precludes FPGS polyglutamation but does not appear to functionally impact transport into the cell.

## Conclusions

To address antifolate resistance derived from reduced FPGS polyglutamation and to avoid the cumulative toxicity of polyglutamylatable antifolates, novel antifolates that act independently of FPGS expression are required. Such derivatives, especially those that act by selective inhibition of the purine biosynthetic pathway, provide the additional opportunity to directly assess their utility in oncology without the complicating features of polyglutamation that often preclude correlations between target affinity and functional activity. For this purpose and in this study, nonpolyglutamatable derivatives of the potent and selective GAR Tfase inhibitor **1**, 10-CF<sub>3</sub>CO-DDACTHF, including **12**, were examined. Like **1**, **12** is transported into the cell and benefits from the action of the reduced folate carrier.

Unlike **1**, the functional activity of **12** is not dependent on FPGS polyglutamation. Thus, not only is **12** only slightly less potent than **1** and approximately 5-fold more potent than lometrexol, but its functional activity is independent of FPGS levels and polyglutamation providing a superb candidate for in vivo examination alongside **1**.

## Experimental Section

**N-((1H-tetrazol-5-yl)methyl)-4-(6-(2,4-diamino-6-oxo-1,6-dihydropyrimidin-5-yl)-1,1,1-trifluoro-2-oxohexan-3-yl)benzamide (8).** A solution of **7** (91 mg, 0.224 mmol) in 1.12 mL of DMF at room temperature was treated with **4** (33 mg, 0.336 mmol), EDCI (86 mg, 0.448 mmol), and NaHCO<sub>3</sub> (42 mg, 0.493 mmol). The solution was stirred for 24 h, followed by concentration and column chromatography (SiO<sub>2</sub>, 70:30:3:3 chloroform/methanol/water/aq ammonium hydroxide). The resulting light yellow oil was triturated with Et<sub>2</sub>O to give **8** (50 mg, 46%) as a light yellow solid: mp 180 °C (dec). <sup>1</sup>H NMR (500 MHz, CD<sub>3</sub>OD)  $\delta$  7.89–7.86 (m, 2H), 7.42–7.40 (m, 2H), 4.82 (s, 2H), 3.15–3.20 (m, 1H), 2.32–2.19 (m, 2H), 2.07–2.04 (m, 2H), 1.30–1.27 (m, 2H); <sup>13</sup>C NMR (125 MHz, CD<sub>3</sub>OD)  $\delta$  192.2, 169.5, 166.9, 165.2, 157.4, 154.9, 152.7, 145.3, 133.2, 131.5 (2C), 128.0 (2C), 90.1, 43.6, 39.6, 37.8, 25.6, 19.3; IR (film)  $\nu_{\max}$  3139, 3045, 1636, 1405 cm<sup>-1</sup>; MALDI-FTMS  $m/z$  480.1722 (M + H<sup>+</sup>, C<sub>19</sub>H<sub>20</sub>F<sub>3</sub>N<sub>9</sub>O<sub>3</sub> requires 480.1714). Analytical HPLC: reversed-phase (acetonitrile/0.1 M ammonium formate/trifluoroacetic acid solution 5:95:0.05, flow rate 1 mL/min);  $t_R$ , 18.0 min; purity, 98.0%.

**tert-Butyl-2-(4-(6-(2,4-diamino-6-oxo-1,6-dihydropyrimidin-5-yl)-1,1,1-trifluoro-2-oxohexan-3-yl)benzamido)acetate (9).** A solution of **7** (90 mg, 0.223 mmol) in 1.12 mL of DMF at room temperature was treated with **5** (56 mg, 0.334 mmol), EDCI (86 mg, 0.446 mmol), and NaHCO<sub>3</sub> (41 mg, 0.491 mmol). The solution was stirred for 24 h, followed by concentration and column chromatography (SiO<sub>2</sub>, 70:30:3:3 chloroform/methanol/water/aq ammonium hydroxide) to give **9** (64 mg, 56%) as a yellow oil. <sup>1</sup>H NMR (500 MHz, CD<sub>3</sub>OD)  $\delta$  7.72 (d, 2H,  $J$  = 8.3 Hz), 7.41 (d, 2H,  $J$  = 8.3 Hz), 4.00 (s, 2H), 3.28–3.11 (m, 1H), 2.42–2.21 (m, 4H), 1.48 (s, 9H), 1.18–1.21 (m, 2H); <sup>13</sup>C NMR (125 MHz, CD<sub>3</sub>OD)  $\delta$  192.0, 171.7, 170.8, 170.6, 165.4, 160.8, 154.9, 145.2, 133.4, 131.3 (2C), 127.8 (2C), 90.0, 82.5, 45.4, 30.0, 29.5, 28.3 (3C), 26.7, 22.9; IR (film)  $\nu_{\max}$  3344, 2978, 2126, 1735, 1624, 1560, 1369, 1226, 1155, 847 cm<sup>-1</sup>; MALDI-FTMS  $m/z$  512.2128 (M + H<sup>+</sup>, C<sub>23</sub>H<sub>28</sub>F<sub>3</sub>N<sub>5</sub>O<sub>5</sub> requires 512.2115).

**2-(4-(6-(2,4-Diamino-6-oxo-1,6-dihydropyrimidin-5-yl)-1,1,1-trifluoro-2-oxohexan-3-yl)benzamido)acetic Acid (10).** A solution of **9** (60 mg, 0.117 mmol) in 1.5 mL of CHCl<sub>3</sub> at 0 °C was treated with 0.75 mL of trifluoroacetic acid. The solution was allowed to warm to room temperature and was stirred for 6 h. Removal of solvent followed by trituration with Et<sub>2</sub>O gave **10** (53 mg, quantitative) as a light yellow solid: mp 108–135 °C. <sup>1</sup>H NMR (500 MHz, CD<sub>3</sub>OD)  $\delta$  7.85 (d, 0.6H,  $J$  = 8.3 Hz), 7.75 (d, 1.4H,  $J$  = 8.3 Hz), 7.41 (d, 1.4H,  $J$  = 8.3 Hz), 7.36 (d, 0.6H,  $J$  = 8.3 Hz), 4.09 (s, 2H), 3.25–3.20 (m, 1H), 2.28–2.23 (m, 1H), 2.15–1.98 (m, 2H), 1.90–1.82 (m, 1H), 1.33–1.21 (m, 2H); <sup>13</sup>C NMR (125 MHz, CD<sub>3</sub>OD)  $\delta$  192.3, 174.2, 173.3, 170.6, 160.8, 153.5, 152.7, 145.1, 133.5, 131.4 (2C), 127.8 (2C), 89.8, 43.5, 42.6, 29.5, 26.8, 22.8; IR (film)  $\nu_{\max}$  3359, 1654, 1199 cm<sup>-1</sup>; MALDI-FTMS  $m/z$  456.1493 (M + H<sup>+</sup>, C<sub>19</sub>H<sub>20</sub>F<sub>3</sub>N<sub>5</sub>O<sub>5</sub> requires 456.1489). Analytical HPLC: reversed-phase (acetonitrile/0.1 M ammonium formate/trifluoroacetic acid solution 5:95:0.05, flow rate 1 mL/min);  $t_R$ , 13.3 min; purity, 98.8%.

**Methyl (2S)-2-(4-(6-(2,4-Diamino-6-oxo-1,6-dihydropyrimidin-5-yl)-1,1,1-trifluoro-2-oxohexan-3-yl)benzamido)-4-(1H-tetrazol-5-yl)butanoate (11).** A solution of **7** (52 mg, 0.129 mmol) in 1.13 mL of DMF was treated with **6** (36 mg, 0.193 mmol), EDCI (50 mg, 0.258 mmol), and NaHCO<sub>3</sub> (24 mg, 0.284 mmol). The solution was stirred for 24 h, followed by concentration and column chromatography (SiO<sub>2</sub>, 70:30:3:3 chloroform/methanol/water/aq ammonium hydroxide) to give **11** (32 mg, 44%) as a light yellow solid: mp 180 °C (dec). <sup>1</sup>H NMR (500 MHz, CD<sub>3</sub>OD)  $\delta$  7.77–

7.74 (m, 2H), 7.43–7.40 (m, 2H), 4.62–4.60 (m, 1H), 3.73 (s, 3H), 3.25–3.22 (m, 1H), 2.97–2.95 (m, 2H), 2.40–2.04 (m, 6H), 1.22–1.19 (m, 2H); <sup>13</sup>C NMR (125 MHz, CD<sub>3</sub>OD) δ 192.1, 174.9, 174.6, 173.5, 161.2, 160.1, 158.2, 155.4, 145.0, 133.1, 131.5 (2C), 128.1 (2C), 90.1, 54.1, 52.8, 43.7, 32.3, 30.5, 24.7, 22.2, 21.2; IR (film) ν<sub>max</sub> 3142, 3047, 1676, 1406 cm<sup>-1</sup>; MALDI–FTMS *m/z* 566.2089 (M + H<sup>+</sup>, C<sub>23</sub>H<sub>26</sub>F<sub>3</sub>N<sub>9</sub>O<sub>5</sub> requires 566.2082).

**(2S)-2-(4-(6-(2,4-Diamino-6-oxo-1,6-dihydropyrimidin-5-yl)-1,1,1-trifluoro-2-oxohexan-3-yl)benzamido)-4-(1H-tetrazol-5-yl)butanoic Acid (12).** A solution of **11** (30 mg, 0.053 mmol) in 1.29 mL of a 2:1 MeOH/THF mixture was treated with 0.5 mL of 1 N aqueous NaOH at room temperature. The solution was stirred for 2 h, followed by removal of organic solvent under vacuum. A 0.5 mL solution of 1 N aqueous HCl was added, followed by concentration and column chromatography (SiO<sub>2</sub>, 70:58:8:8 chloroform/methanol/water/aq ammonium hydroxide) to give **12** (7.3 mg, 25%) as a light yellow solid: mp 170 °C (dec). <sup>1</sup>H NMR (500 MHz, CD<sub>3</sub>OD) δ 7.76–7.72 (m, 2H), 7.41–7.37 (m, 2H), 4.55–4.57 (m, 1H), 3.10–2.95 (m, 3H), 2.40–2.21 (m, 4H), 2.09–1.91 (m, 2H), 1.25–1.18 (m, 2H); <sup>13</sup>C NMR (125 MHz, CD<sub>3</sub>OD) δ 191.5, 181.7, 176.1, 174.6, 164.0, 159.2, 157.3, 153.2, 145.6, 133.8, 131.2 (2C), 127.7 (2C), 88.1, 55.3, 43.6, 30.8, 30.6, 26.5, 23.0, 20.7; IR (film) ν<sub>max</sub> 3127, 3038, 1654, 1400 cm<sup>-1</sup>; MALDI–FTMS *m/z* 552.1926 (M + H<sup>+</sup>, C<sub>22</sub>H<sub>24</sub>F<sub>3</sub>N<sub>9</sub>O<sub>5</sub> requires 552.1925). Analytical HPLC: reversed-phase (acetonitrile/0.1 M ammonium formate/trifluoroacetic acid solution 5:95:0.05, flow rate 1 mL/min); *t<sub>R</sub>*, 10.5 min; purity, 96.7%.

**GAR and AICAR Tfase Assay.** Enzyme assays for rhGAR and rhAICAR were performed as described previously.<sup>19,24</sup> Kinetics of the enzyme reactions were monitored for 2 min after initiation of the reaction. *K<sub>i</sub>*'s of the inhibitors were calculated using Dixon plots.

**Cytotoxic Assay.** The cytotoxic activity of the compounds was measured using the CCRF–CEM human leukemia cell lines as described previously.<sup>19,23,24,26</sup>

## Abbreviations

GAR Tfase, glycinamide ribonucleotide transformylase; rhGAR Tfase, recombinant human GAR Tfase; FPGS, folic polyglutamate synthase; 10-formyl-THF, 10-formyltetrahydrofolic acid; MTX, methotrexate; MTAP, methylthioadenosine phosphorylase; AICAR Tfase, aminoimidazole carboxamide ribonucleotide transformylase; rhAICAR Tfase, recombinant human AICAR Tfase; DDACTHF, dideaza-acyclic-cyclotetrahydrofolic acid; EDCl, 1-(3-dimethylaminopropyl)-3-ethylcarbodiimide.

**Acknowledgment.** We gratefully acknowledge the financial support of the National Institutes of Health (CA63536) and the Skaggs Institute for Chemical Biology. J.K.D. is a Skaggs Fellow.

## References

- Warren, L.; Buchanan, J. M. 2-Amino-*N*-ribosylacetamide 5'-phosphate (glycinamide ribotide) transformylase. *J. Biol. Chem.* **1957**, *229*, 1979–1992.
- Dev, I. K.; Harvey, R. J. N10-Formyltetrahydrofolate is the formyl donor for glycinamide ribonucleotide transformylase in *Escherichia coli*. *J. Biol. Chem.* **1978**, *253*, 4242–4244.
- Kamatani, N.; Nelson-Rees, W. A.; Carson, D. A. Selective killing of human malignant cell lines deficient in methylthioadenosine phosphorylase, a purine metabolic enzyme. *Proc. Natl. Acad. Sci. U.S.A.* **1981**, *78*, 1219–1223. See also: (b) Hori, H.; Tran, P.; Carrera, C. J.; Hori, Y.; Rosenbach, M. D.; Carson, D. A.; Nobori, T. Methylthioadenosine phosphorylase cDNA transfection alters sensitivity to depletion of purine and methionine in A549 lung cancer cells. *Cancer Res.* **1996**, *56*, 5653–5658.
- Gordon, R. B.; Blackwell, K.; Emmerson, B. T. Synthesis of purines in human lymphoblast cells deficient in methylthioadenosine phosphorylase activity. *Biochim. Biophys. Acta* **1987**, *927*, 1–7.
- Efferth, T.; Miyachi, H.; Drexler, H. G.; Gebhart, E. Methylthioadenosine phosphorylase as target for chemoselective treatment of T-cell acute lymphoblastic leukemic cells. *Blood Cells, Mol. Dis.* **2002**, *28*, 47–56.
- Chen, Z. H.; Olopade, O. I.; Savarese, T. M. Expression of methylthioadenosine phosphorylase cDNA in *p16*<sup>-</sup>, *MTAP*<sup>-</sup> malignant cells: restoration of methylthioadenosine phosphorylase-dependent salvage pathways and alterations of sensitivity to inhibitors of purine de novo synthesis. *Mol. Pharmacol.* **1997**, *52*, 903–911.
- Gibbs, D.; Jackman, A.; Kirkpatrick, P. Pemetrexed disodium. *Nat. Rev. Drug Discovery* **2005**, *4*, S16–S17.
- McCloskey, D. E.; McGuire, J. J.; Russel, C. A.; Rowan, B. G.; Bertino, J. R.; Pizzorno, G.; Mini, E. J. Decreased folypolyglutamate synthase activity as a mechanism of methotrexate resistance in CCRF–CEM human leukemia sublines. *J. Biol. Chem.* **1991**, *266*, 6181–6187.
- Wang, Y.; Zhao, R.; Goldman, I. D. Decreased expression of the reduced folate carrier and folypolyglutamate synthetase is the basis for acquired resistance to the pemetrexed antifolate (LY231514) in an L1210 murine leukemia cell line. *Biochem. Pharmacol.* **2003**, *65*, 1163–1170.
- Laohaviniij, S.; Wedge, S. R.; Lind, M. J.; Bailey, N.; Humphreys, A.; Proctor, M.; Chapman, F.; Simmons, D.; Oakley, A. A phase I clinical study of the antipurine folate lometrexol (DDATHF) given with oral folic acid. *Invest. New Drugs* **1996**, *14*, 325–335.
- Balinska, M.; Nimec, Z.; Galivan, J. Characteristics of methotrexate polyglutamate formation in cultured hepatic cells. *Arch. Biochem. Biophys.* **1982**, *216*, 466–476.
- Marsham, P. R.; Wardleworth, J. M.; Boyle, F. T.; Hennequin, L. F.; Kimbell, R.; Brown, M.; Jackman, A. L. Design and synthesis of potent nonpolyglutamatable quinazoline antifolate thymidylate synthase inhibitors. *J. Med. Chem.* **1999**, *42*, 3809–3820.
- Webber, S. E.; Bleckman, T. M.; Attard, J.; Deal, J. G.; Kathardekar, V.; Welsh, K. M.; Webber, S.; Janson, C. A.; Matthews, D. A.; Smith, W. W.; Freer, S. T.; Jordan, S. R.; Bacquet, R. J.; Howland, E. F.; Booth, C. L. J.; Ward, R. W.; Hermann, S. M.; White, J.; Morse, C. A.; Hilliard, J. A.; Bartlett, C. A. Design of thymidylate synthase inhibitors using protein crystal structures: the synthesis and biological evaluation of a novel class of 5-substituted quinazolinones. *J. Med. Chem.* **1993**, *36*, 733–746.
- Itoh, F.; Yukishige, K.; Wajima, M.; Ootsu, K.; Akimoto, H. Nonglutamate type pyrrolo[2,3-*d*]pyrimidine antifolates. I: Synthesis and biological properties of pyrrolo[2,3-*d*]pyrimidine antifolates containing tetrazole congeners of glutamic acid. *Chem. Pharm. Bull.* **1995**, *43*, 230–235.
- Kisliuk, R. L. Deaza analogues of folic acid as antitumor agents. *Curr. Pharm. Des.* **2003**, *9*, 2615–2625.
- Antonjuk, D. J.; Boadle, D. K.; Cheung, H. T. A.; Tran, T. Q. Synthesis of monoamides of methotrexate from L-glutamic acid monoamide *tert*-butyl esters. *J. Chem. Soc., Perkin Trans. 1* **1984**, 1989–2003.
- Rosowsky, A.; Forsch, R. A.; Null, A.; Moran, R. G. 5-Deazafolate analogues with a rotationally restricted glutamate or ornithine side chain: synthesis and binding interaction with folypolyglutamate synthetase. *J. Med. Chem.* **1999**, *42*, 3510–3519.
- Vaidya, C. M.; Wright, J. E.; Rosowsky, A. Synthesis and in vitro antitumor activity of new deaza analogues of the nonpolyglutamatable antifolate *N*<sup>6</sup>-(4-amino-4-deoxypteroyl)-*N*<sup>10</sup>-hemipthaloyl-L-ornithine (PT523). *J. Med. Chem.* **2002**, *45*, 1690–1696.
- Zhang, Y.; Desharnais, J.; Marsilje, T. H.; Li, C.; Hedrick, M. P.; Gooljarsingh, L. T.; Tavassoli, A.; Benkovic, S. J.; Olson, A. J.; Boger, D. L.; Wilson, I. A. Rational design, synthesis, evaluation, and crystal structure of a potent inhibitor of human GAR Tfase: 10-trifluoroacetyl-5,10-dideaza-acyclic-5,6,7,8-tetrahydrofolic acid. *Biochemistry* **2003**, *42*, 6043–6056.
- Desharnais, J.; Hwang, I.; Zhang, Y.; Tavassoli, A.; Baboval, J.; Benkovic, S. J.; Wilson, I. A.; Boger, D. L. Design, synthesis, and biological evaluation of 10-CF<sub>3</sub>CO-DDACTHF analogues and derivatives as inhibitors of GAR Tfase and the de novo purine biosynthetic pathway. *Bioorg. Med. Chem.* **2003**, *11*, 4511–4521.
- Chong, Y.; Hwang, I.; Tavassoli, A.; Zhang, Y.; Wilson, I. A.; Benkovic, S. J.; Boger, D. L. Synthesis and biological evaluation of α- and γ-carboxamide derivatives of 10-CF<sub>3</sub>CO-DDACTHF. *Bioorg. Med. Chem.* **2005**, *13*, 3587–3592.
- Demko, Z.; Sharpless, K. B. An expedient route to the tetrazole analogues of α-amino acids. *Org. Lett.* **2002**, *4*, 2525–2527.
- Bigham, E. C.; Hodson, S. J.; Mallory, W. R.; Wilson, D.; Duch, D. S.; Smith, G. K.; Ferone, R. Synthesis and biological activity of open-chain analogues of 5,6,7,8-tetrahydrofolic acid-potential antitumor agents. *J. Med. Chem.* **1992**, *35*, 1399–1410.
- Marsilje, T. H.; Labroli, M. A.; Hedrick, M. P.; Jin, Q.; Desharnais, J.; Baker, S. J.; Gooljarsingh, L. T.; Ramcharan, J.; Tavassoli, A.; Zhang, Y.; Wilson, I. A.; Beardley, G. P.; Benkovic, S. J.; Boger, D. L. 10-Formyl-5,10-dideaza-acyclic-5,6,7,8-tetrahydrofolic acid (10-formyl-DDACTHF): A potent cytotoxic agent acting by selective inhibition of human GAR Tfase and the de novo purine biosynthetic pathway. *Bioorg. Med. Chem.* **2002**, *10*, 2739–2749.

- (25) Habeck, L. L.; Leitner, T. A.; Shackelford, K. A.; Gossett, L. S.; Schultz, R. M.; Andis, S. L.; Shih, C.; Grindey, G. B.; Mendelsohn, L. G. A novel class of monoglutamated antifolates exhibits tight-binding inhibition of human glycinamide ribonucleotide formyltransferase and potent activity against solid tumors. *Cancer Res.* **1994**, *54*, 1021–1026.
- (26) This assay, as is standard, was conducted with 72 h of continuous exposure to the candidate inhibitors. It has been reported that nonpolyglutamatable antifolates may exhibit lower potency under short exposure (6 h) conditions due to rapid efflux from the cells. This was not examined with **10–12** herein. See: (a) McGuire, J. J.; Russell, C. A.; Bolanowska, W. E.; Freitag, C. M.; Jones, C. S.;

Kalman, T. I. Biochemical and growth inhibition studies with methotrexate and aminopterin analogues containing a tetrazole ring in place of the  $\gamma$ -carboxyl group. *Cancer Res.* **1990**, *50*, 1726–1731.

(b) Jackman, A. L.; Kimbell, R.; Aherne, G. W.; Brunton, L.; Jansen, G.; Stephens, T. C.; Smith, M. N.; Wardleworth, J. M.; Boyle, F. T. Cellular pharmacology and in vivo activity of a new anticancer agent ZD9331: a water soluble, nonpolyglutamatable, quinazoline-based inhibitor of thymidylate synthase. *Clin. Cancer Res.* **1997**, *3*, 911–921.

JM0601147